

Broad-Range Modulation of Light Emission in Two-Dimensional Semiconductors by Molecular Physisorption Gating

Sefaattin Tongay,^{†,¶} Jian Zhou,^{†,¶} Can Ataca,[‡] Jonathan Liu,[†] Jeong Seuk Kang,[†] Tyler S. Matthews,[†] Long You,[§] Jingbo Li,^{||} Jeffrey C. Grossman,[‡] and Junqiao Wu^{*,†,⊥}

[†]Department of Materials Science and Engineering, University of California, Berkeley, California 94720, United States

[‡]Department of Materials Science and Engineering, Massachusetts Institute of Technology, Cambridge, Massachusetts 02139, United States

[§]Department of Electrical Engineering and Computer Sciences, University of California, Berkeley, California 94720, United States

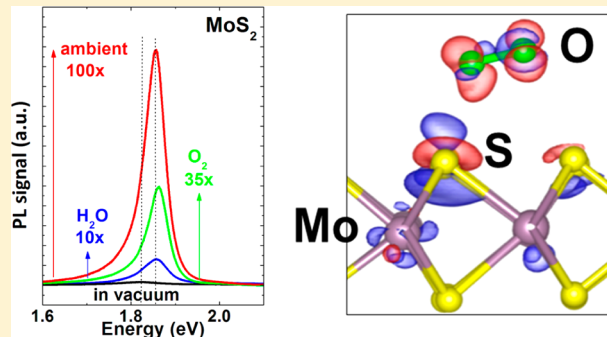
^{||}Institute of Semiconductors, Chinese Academy of Sciences, P.O. Box 912, Beijing 100083, People's Republic of China

[⊥]Materials Sciences Division, Lawrence Berkeley National Laboratory, Berkeley, California 94720, United States

Supporting Information

ABSTRACT: In the monolayer limit, transition metal dichalcogenides become direct-bandgap, light-emitting semiconductors. The quantum yield of light emission is low and extremely sensitive to the substrate used, while the underlying physics remains elusive. In this work, we report over 100 times modulation of light emission efficiency of these two-dimensional semiconductors by physical adsorption of O₂ and/or H₂O molecules, while inert gases do not cause such effect. The O₂ and/or H₂O pressure acts quantitatively as an instantaneously reversible “molecular gating” force, providing orders of magnitude broader control of carrier density and light emission than conventional electric field gating. Physisorbed O₂ and/or H₂O molecules electronically deplete n-type materials such as MoS₂ and MoSe₂, which weakens electrostatic screening that would otherwise destabilize excitons, leading to the drastic enhancement in photoluminescence. In p-type materials such as WSe₂, the molecular physisorption results in the opposite effect. Unique and universal in two-dimensional semiconductors, the effect offers a new mechanism for modulating electronic interactions and implementing optical devices.

KEYWORDS: 2D semiconductors, optical emission, charge transfer, excitons, molecular physisorption



Layered transition metal dichalcogenides (TMDs) with the chemical formula MX₂ (M = Mo, W, Ru and X = S, Se, and Te) display a wide range of attractive physical and chemical properties^{1–5} and are potentially important for device applications.⁶ Several semiconducting MX₂ show an indirect-to-direct bandgap transition going from the bulk to monolayer. For instance, monolayers of MoS₂,¹ MoSe₂,⁷ WS₂,^{8,9} and WSe₂^{8,9} have direct bandgaps ranging from 1.5 to 2.0 eV. Unusual physical effects, such as valley-selective electronics^{3–5} and charged exciton stabilization,^{10,11} have been recently observed in monolayer TMDs. Considering the wide range of direct bandgap values available, semiconducting MX₂ in the monolayer limit are especially promising for two-dimensional (2D) optoelectronics, such as light-emitting diodes and optical energy conversion devices.

However, the PL quantum yield of monolayer MX₂ has been found to be low in monolayers.² The light-emitting efficiency of these monolayers is highly susceptible to boundary conditions such as the substrate in which they are placed.^{2,4} In this work, we demonstrate an unprecedentedly wide range of modulation

of PL intensity in monolayer TMDs by exposing the sample to O₂ and/or H₂O gas. The modulation is completely, quantitatively reversible at room temperature by simply controlling the gas pressure, indicating that physisorption of the gas molecules is responsible for the modulation. Inert gases such as Ar and N₂ do not affect the PL intensity. Density functional theory (DFT) calculations discover that the O₂ and H₂O molecules interact weakly to the TMD monolayers with binding energies ranging from 70 to 140 meV and withdraw a substantial number of electrons from the latter. The charge transfer depletes n-type TMDs (MoS₂ and MoSe₂) and stabilizes excitons that would be otherwise screened; consequently a new radiative recombination channel is activated, resulting in a remarkable enhancement in the PL intensity. In contrast, the O₂ and H₂O molecules accumulate the majority holes in p-type TMDs (WSe₂), resulting in strong

Received: March 27, 2013

Revised: April 25, 2013

Published: April 29, 2013

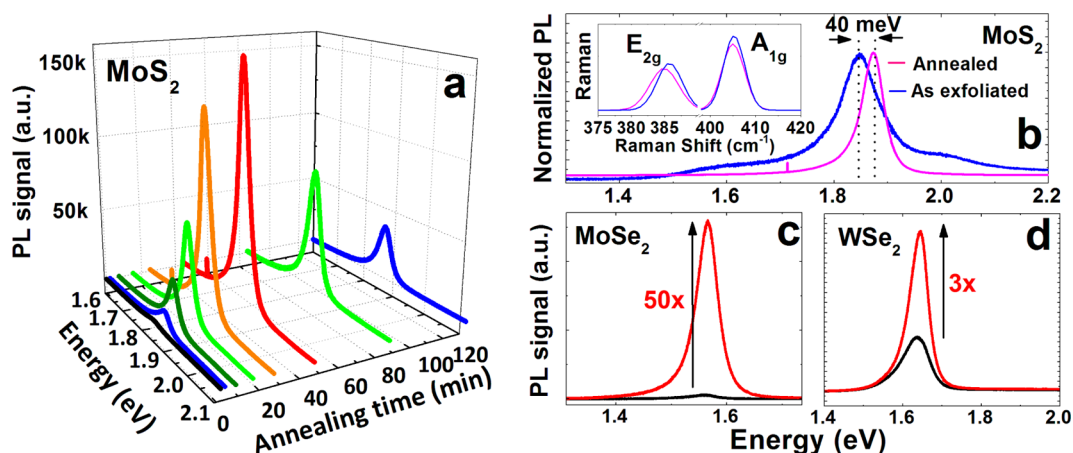


Figure 1. Drastic enhancement in room-temperature photoluminescence intensity of monolayer TMDs by thermal annealing. (a) PL spectrum of monolayer MoS₂ as a function of annealing time. The anneal is at 450 °C in vacuum. The laser excitation intensity is fixed at 4×10^4 W/m² for the PL measurements. (b) Normalized PL spectrum for pristine and optimally annealed monolayer MoS₂. (Inset) Raman spectrum of pristine and annealed monolayer MoS₂. (c) PL intensity enhancement of monolayer MoSe₂ upon thermal anneal at 250 °C for 15 min. The peak is blue shifted by ~ 17 meV. (d) PL intensity enhancement of monolayer WSe₂ upon thermal anneal at 300 °C for 10 min. The peak shift is blue shifted by ~ 10 meV. All the PL measurements are taken at room temperature in ambient condition.

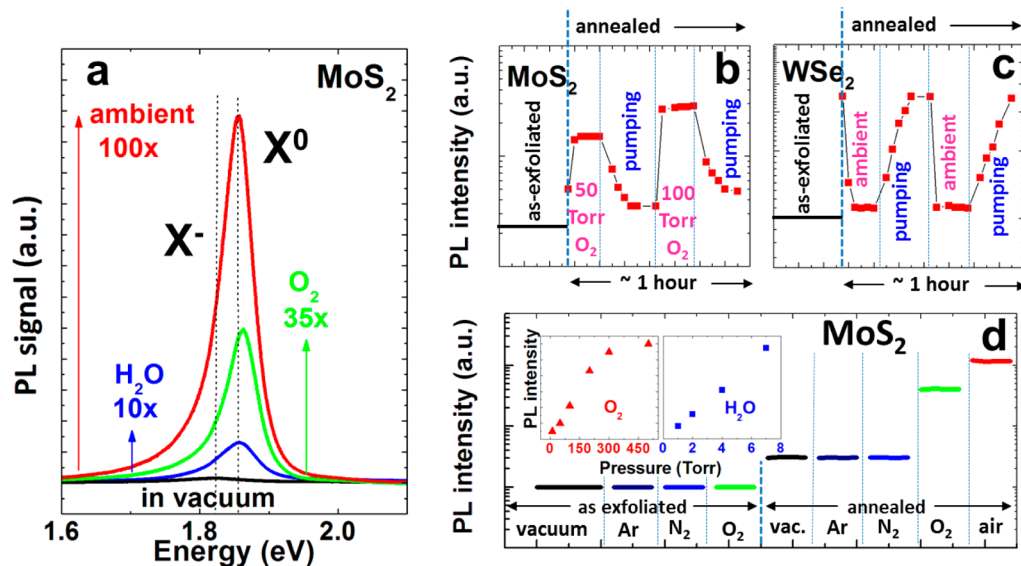


Figure 2. Effects of exposure to different gas species on the PL intensity of annealed monolayer TMDs. (a) Change in PL of MoS₂ (from its annealed but measured in vacuum value) upon exposure to H₂O alone, O₂ alone, and ambient air. The pressure of these gases is 7, 200, and 760 Torr, respectively. Trion X⁻ and exciton X⁰ peak positions are indicated. (b) Modulation of the PL intensity of monolayer MoS₂ as a function of O₂ purging (50 and 100 Torr, respectively) and pumping. (c) Modulation of the PL intensity of monolayer WSe₂ as a function of ambient air purging (760 Torr) and pumping. Note the opposite response in MoS₂ and WSe₂. The time periods of purging and pumping in panels b and c are on the order of minutes. (d) Effect of Ar, N₂, O₂, and air on the PL intensity of annealed and as-exfoliated monolayer MoS₂. Inset: PL intensity as a function of O₂ and H₂O pressure. Note the log scale of PL intensity in panels b, c, and d.

suppression of the PL. In addition to the PL intensity modulation, the PL peak position also slightly shifts, which is explained by a switch between neutral exciton recombination and charged exciton (trion) recombination. The molecular physisorption, acting as a gating force, provides much wider control of charge density and light emission than conventional electric field gating and is free of limitations in the latter that are imposed by dielectric breakdown, metal contacts, and device fabrication. Such results and understanding not only shed new light on many-body physics in 2D semiconductors but also provides a foundation for new optoelectronic devices where strong PL modulation by external means is desired.

Annealing and Molecular Physisorption Effects. The TMD flakes were mechanically exfoliated from bulk crystals (see Methods) onto 90 nm thick thermal silicon oxide where a relatively high contrast can be observed for the flakes.¹² Monolayer TMD typically displays a thickness of ~ 0.7 nm as determined by atomic force microscopy (AFM). The monolayers could also be identified by other complementary methods such as microscale Raman spectroscopy and PL measurements (see Supporting Information). From bulk to monolayers, the out-of-plane Raman mode (A_{1g}) softens while the in-plane mode (E_{2g}) stiffens.¹³ Consistent with previous reports,^{1,2} stronger PL is observed from monolayer TMDs compared to its multilayer and bulk counterparts. At room

temperature, monolayer MoS₂, MoSe₂, and WSe₂ show a prominent PL peak at ~1.84, 1.56, and 1.63 eV, respectively.

To attain the sensitivity to gas molecules, an anneal-based “forming process” is needed for as-exfoliated TMD monolayers. Here, the forming process can be pictured as a process to expose the monolayer surface to the ambient by thermally driving away contaminants/organic residue, which is similar to the sample preparation techniques commonly used for scanning tunneling microscopy or releasing stress built in the monolayers by the substrate. Another possibility is that the forming process might be creating a small density of chalcogen vacancies in the monolayer (Figure S3 in Supporting Information). Figure 1a shows PL spectrum of a monolayer MoS₂ measured at room temperature after 450 °C anneal in vacuum for different annealing times. A 40 min anneal at 450 °C enhances the PL intensity by over 50 times, while the full width at half-maximum (fwhm) of the PL peak decreases from 90 to 45 meV, and the PL peak position shifts from ~1.84 to ~1.88 eV, as shown in the normalized PL plot (Figure 1b). A comparison between the Raman spectrum of pristine (i.e., as-exfoliated) and optimally annealed monolayer MoS₂ (Figure 1b inset) shows that the fwhm and peak intensity of the A_{1g} and E_{2g} peaks remain largely unchanged, therefore the thermal anneal does not degrade the crystalline quality of the material. However, the in-plane Raman mode (E_{2g}) softens from 384.5 to 383 cm⁻¹, possibly attributed to desorption of contamination molecules and/or releasing stress on the monolayers. This change is irreversible; that is, subsequent treatments (further annealing and pumping/purging of gas) do not cause further changes to the Raman spectrum. We found that 40 min anneal at 450 °C optimally enhances the PL intensity. The enhancement is less for both weaker (shorter times or lower temperatures) and stronger annealing (longer times or higher temperatures). This is a general effect, as other 2D semiconductors, monolayer MoSe₂ and WSe₂ (Figure 1c,d), also exhibits similar behavior but with different optimal annealing condition.

After the forming process, the photoluminescence intensity of monolayer TMDs becomes extremely sensitive to gas environment. In the following discussion, we first focus on MoS₂. Immediately after annealing, the MoS₂ was transferred into a vacuum chamber for micro-PL measurements. The chamber was pumped down to 10⁻⁴ Torr prior to backfilling with different gases at controlled pressures. As shown in Figure 2a, upon exposing the MoS₂ to H₂O alone (7 Torr), O₂ alone (200 Torr), or O₂ and H₂O together, the PL intensity was enhanced by 10, 35, and 100 times, respectively. When the gas pressure changes, the PL intensity also changes instantaneously, and the time it takes for the MoS₂ to reach the new PL intensity is merely limited by the pumping/purging speed and the time needed for the PL measurement, as shown in Figure 2b. The PL remains constant over a time frame of days, as long as the gas pressure stays constant. Pumping the O₂ or H₂O gas out of the chamber, the PL intensity immediately reverts back to its original value (i.e., postanneal PL measured in vacuum), implying that the O₂ and H₂O molecules are physisorbed, as opposed to chemisorbed, on the MoS₂ surface. The PL can be reversibly modulated for numerous times by pumping and purging with O₂ and/or H₂O. The PL intensity is nearly linearly proportional to the O₂ or H₂O pressure, as shown in the inset of Figure 2d. This is consistent with the physisorption picture of molecules, because in equilibrium sheet density of physisorbed molecules on the surface is proportional to the gas pressure. Above a particular O₂ pressure (Figure 2d inset), the

PL intensity displays a tendency to saturate. This threshold value depends possibly on the average distance between the physisorbed O₂ molecules, which determines the largest effective area where O₂ can interact with the MoS₂. For the H₂O experiment, the pressure cannot be increased more than 7 Torr due to instrumental limitations, and in the 0–7 Torr range such saturation in PL enhancement was not observed. Exposing the annealed MoS₂ to inert gases of Ar or N₂ does not change its PL intensity (Figure 2d); therefore, the PL enhancement must be attributed to the molecular property of O₂ and H₂O interacting with MoS₂. We also note that when both O₂ and H₂O interacts with MoS₂ (in ambient air), the PL enhancement surpasses that of O₂ or H₂O alone, as the different types of gas molecules simultaneously deplete the monolayer. More interestingly, while MoSe₂ exhibits similar gas sensitivity (not shown here) as MoS₂, WSe₂ shows the opposite behavior (Figure 2c); that is, exposing to O₂ and/or H₂O strongly suppresses the PL of monolayer WSe₂.

Density Functional Theory Calculations. To provide a physical picture for the effect of O₂ and H₂O, we simulated the interaction between monolayer MoS₂ and O₂ or H₂O molecules using density functional theory (DFT) calculations. Calculating the van der Waals energy between the molecule and MoS₂ as a function of angle and distance reveals that O₂ and H₂O molecules can be physisorbed on the MoS₂ surface with 79 and 110 meV binding energies, respectively. Once physisorbed, the O₂ or H₂O molecule is blocked from chemisorption by a high energy barrier (~2 eV), but approximately 0.04 electrons per O₂ and 0.01 electrons per H₂O are transferred to the molecules, depleting the monolayer MoS₂, as shown in Figure 3a,b. Because of the monolayer thickness of the MoS₂, the total number of charge transferred from the MoS₂ to the gas molecules adds up to remarkably high

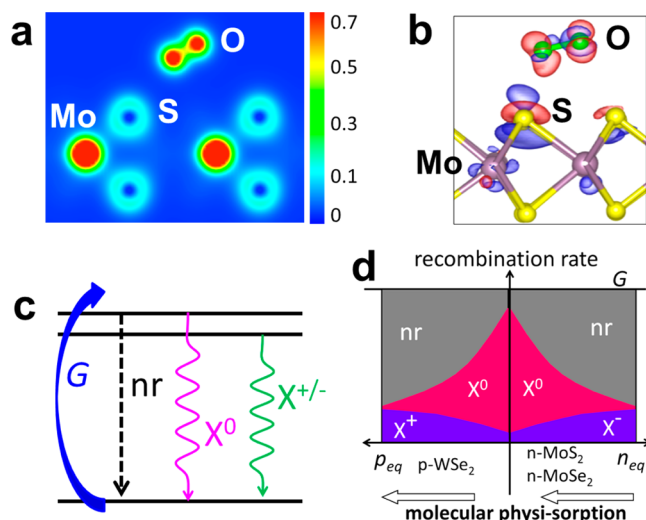


Figure 3. Recombination and charge transfer under physisorbed O₂ or H₂O. (a) Charge density distribution of an O₂ molecule physisorbed on the MoS₂ surface. The color scale is in the units of e/Å³. (b) Charge density difference between pristine MoS₂ and O₂-adsorbed MoS₂. The iso-surface is for electron density of 2 × 10⁻⁴ e/Å³. Red is charge accumulation and blue is charge depletion. (c) Schematic of the excitation and recombination process. The nonradiative recombination, exciton recombination, and trion recombination are represented by the process of nr, X⁰, and X⁻, respectively. (d) Rate of nr, X⁰, and X⁻ (or X⁺) as a function of equilibrium electron density in n- (or p-) type 2D semiconductors.

sheet densities. Assuming that one O₂ molecule is physisorbed on each unit cell of MoS₂, the charge transfer would reduce the original sheet carrier density as much as $5 \times 10^{13}/\text{cm}^2$. This number can reach even higher values if the physisorption occurs at defect sites where the charge transfer is higher. For example, we find that the O₂ and H₂O molecules bind more strongly at sulfur-vacancy sites (110 meV for O₂ and 150 meV for H₂O), and for H₂O the charge transfer per molecules increases by a factor of 5.

Discussion. The observations in Figures 1 and 2 can be summarized as a drastic enhancement in PL intensity accompanied with a peak shift from 1.84 to 1.88 eV when the monolayer MoS₂ is electrically depleted of free electrons. Compared with literature data,¹⁰ the high-energy peak at ~ 1.88 eV is associated with recombination of neutral excitons (X⁰), while the low-energy peak at 1.84 eV with negatively charged excitons (trion, X⁻), that is, an electron bound to a neutral exciton. The energy difference of ~ 40 meV is attributed to the binding energy (E_{b1}) of the second electron in X⁻. It has been predicted that due to a higher E_{b1} , it is much easier to observe radiative recombination of trions in quantum confined systems.¹⁴ Values of E_{b1} ranging from 2 to 6 meV were reported for semiconductor quantum dots and quantum wells at temperatures typically below 10 K.^{15–19} It was recently reported to be ~ 40 meV for ungated monolayer MoS₂ at 14K,^{4,10} and 30 meV for monolayer MoSe₂ at 20K.¹¹ In those experiments, the relative PL intensities of X⁻ and X⁰ could be slightly tuned by electrostatically controlling the charge state of the material.

The as-exfoliated MoS₂ is known to be unintentionally n-type doped^{4,6,10} with a high sheet density of equilibrium electrons (n_{eq}) up to $10^{13}/\text{cm}^2$. The rate equation of nonequilibrium free electrons (n) under photoexcitation and recombination is

$$\frac{dn}{dt} = G - \frac{n \cdot \eta_{X^0}}{\tau_{\text{nr}}} - \frac{n \cdot \eta_{X^0}}{\tau_{X^0}} - \frac{n \cdot \eta_{X^-}}{\tau_{X^-}} \quad (1)$$

where G is the photoexcitation rate, and the subscription “nr”, “X⁰” and “X⁻” stands for nonradiative (including defects-mediated and Auger process), neutral exciton radiative, and trion radiative recombination process, respectively. τ is recombination lifetime; η is the probability of an electron falling into one of these three pathways (Figure 3c), which satisfies $\eta_{\text{nr}} + \eta_{X^0} + \eta_{X^-}$. In the presence of high n_{eq} , the probability of forming X⁰ and X⁻ (i.e., η_{X^0} and η_{X^-}) is expected to rapidly decrease due to electrostatic screening between free electrons and holes,¹⁸ on the other hand, high n_{eq} favors formation of X⁻ (but not X⁰) by providing the second electron for trions. As a result, η_{X^-} and η_{X^0} have very different functional dependence on n and n_{eq} . In steady state, the n_{eq} dependence of the rate of nonradiative recombination, exciton radiative, and trion radiative recombination is schematically shown in Figure 3d. It can be seen that for as-exfoliated monolayer MoS₂ where n_{eq} is high, X⁰ is destabilized due to charge screening while X⁻ recombination is relatively high due to the abundance of free electrons. The total radiation intensity is low, because most photoexcited electrons and holes are forced to recombine nonradiatively; The nonradiative recombination may be dominated by the Auger process at such high n_{eq} . As the monolayer MoS₂ physisorbs electronegative molecules such as O₂ and H₂O, n_{eq} is much depleted by the charge transfer. Consequently, X⁰ is stabilized while X⁻ is depleted, resulting in a high intensity of X⁰ and a diminishing X⁻ peak in the PL

spectrum. Therefore, the modulation of PL between the X⁰ peak at 1.88 eV and X⁻ peak at 1.84 eV is a direct result of competition between charge screening that destabilizes both excitons and trions, and charge accumulation that is needed for trions but not for excitons. We note that the tail at the low-energy shoulder of the X⁰ PL peaks in Figure 2a is probably caused by disorder and defects, as is in conventional semiconductors. It is not attributed to a residual X⁻ signal, which is overshadowed by the much stronger X⁰.

The behavior of recombination rates in Figure 3d is consistent with the recent report by Mak et al.¹⁰ that at low temperature the X⁰ emission intensity is gate voltage dependent, while that of X⁻ is mostly gate voltage independent. It is not surprising that electric field gating (in vacuum) has a much weaker effect on the PL intensity than molecular physisorption, because the modulation range of sheet carrier density by gate field is typically well below $10^{13}/\text{cm}^2$, limited by breakdown of the gating dielectric. The reversible physisorption acts as a kind of “molecular gating” to withdraw a large density of electrons and drastically modulate the PL. At subatmosphere gas pressures, the molecular gating can easily modulate the sheet carrier density much beyond the dielectric breakdown point that limits conventional electric field gating.

The understanding can be generalized to other monolayer TMDs. We find that after the anneal-forming process, MoSe₂ behaves very similarly to MoS₂ in the interaction with O₂/H₂O, while WSe₂ shows the opposite behavior (Figure 2c). The PL intensity of WSe₂ is the highest when measured in vacuum and suppressed by the presence of O₂ and/or H₂O. This is understood considering that as-exfoliated WSe₂ is p-type,²⁰ while MoS₂ and MoSe₂ are both n-type. The different types of native doping are related to the high-lying valence band maximum of WSe₂ and low-lying conduction band minimum of MoS₂ and MoSe₂.²¹ Therefore, the electron transfer to O₂ or H₂O molecules depletes the majority (electrons, n_{eq}) in MoS₂ and MoSe₂ but accumulates the majority (holes, p_{eq}) in WSe₂. As a result, the PL intensity of X⁰ is reduced by physisorption of O₂/H₂O in WSe₂, as shown schematically in Figure 3d. The PL peak shift in Figure 1c,d gives a room-temperature binding energy of negative trion X⁻ ~ 17 meV in MoSe₂, and of positive trion X⁺ ~ 10 meV in WSe₂.

Lastly, we emphasize that the charge transfer between the gas molecules and the monolayer MX₂ is the most important factor in PL modulation. The annealing is only a necessary prestep to activate the molecule adsorption. The reported PL modulation might be enhanced even more by activating N₂ molecules in air, so that they also transfer charges with the monolayer, as O₂ molecules do. One way to achieve this is to intentionally create point defects in the monolayer, where the electronic interaction with N₂ molecules is artificially activated. It is also possible to enhance the charge transfer by modifying the MX₂ surface with chemical agents that sensitize the surface to gas molecules.

Conclusions. In summary, we have shown a universal effect that the light emission efficiency in 2D semiconductors is dominated by charge transfer to physically adsorbed electro-negative gas molecules such as O₂ and H₂O. The process is unique in such 2D system not only because of its high surface area that is prone to interactions with gaseous molecules, but also its 2D nature that stabilizes many-body exciton effects. The effect not only enables reversible, quantitative control of light emission intensity with gas pressure as a gating force, a desired function for new applications such as sensors, phosphors, and optical switch, but also highlights the importance of interaction

with gases/ambient air that greatly affects the optical properties of monolayer TMDs.

Methods. *Sample Preparation and Micro-PL/Raman Measurements.* Monolayer MoX₂ flakes were exfoliated from bulk crystals (2D semiconductors and SPI) onto p-type Si wafer (MTI corporation, resistivity 0.001–0.1 Ωcm) with 90 nm thermal oxide. Measurements were performed using a Renishaw micro-PL/Raman system. The laser beam (wavelength 488 nm) was focused onto the sample (spot diameter of ~1–2 μm) using excitation power up to 2–5 μW. The PL/Raman measurements in different gas conditions were performed in a homemade vacuum chamber pumped down to ~10⁻⁴ Torr using a turbo-molecular pump. O₂, Ar, or N₂ gas was introduced into the chamber regulated by flow meters and the pressure was measured by a vacuum gauge. The effect of H₂O was tested by electrically heating up a quartz crucible of deionized water near the sample to create a H₂O-rich environment.

Thermal Annealing. The samples were heated to 450 °C in a 30 °C/min rate and the temperature was held at 450 ± 0.1 °C for different duration times. The annealing was performed in a 2 in. quartz tube in vacuum (30 mTorr base pressure). Prior to the annealing, the quartz tube was cleaned at 1000 °C in H₂ gas (2 Torr) for a couple hours. After annealing, the furnace was cooled down to room temperature at a fast rate and the samples were taken out of the furnace and immediately transferred to the Raman chamber for optical measurements.

Density Functional Theory Calculations. Our calculations were based on first-principles DFT using projector-augmented wave potentials.²² The exchange correlation potential has been represented by the generalized gradient approximation characterized by Perdew–Burke–Ernzerhof²³ including van der Waals corrections²⁴ both for spin-polarized and spin-unpolarized cases. Effects of spin–orbit coupling and noncollinear magnetism were taken into account in the spin-polarized calculations. The supercell size, kinetic energy cutoff, and Brillouin zone sampling of the calculations were determined after extensive convergence analyses. A large spacing of ~15 Å between the 2D single layers was used to prevent interlayer interactions. A plane-wave basis set with kinetic energy cutoff of 300 eV was used. In the self-consistent field potential and total energy calculations, the Brillouin zone was sampled by special *k*-points. The numbers of these *k*-points were (25 × 25 × 1) and (15 × 15 × 5) for the primitive 1H-MoS₂ and were scaled according to the size of the super cells. All atomic positions and lattice constants were optimized using the conjugate gradient method, where the total energy and atomic forces were minimized. The convergence for energy were chosen to be 10⁻⁶ eV between two consecutive steps, and the maximum Hellmann–Feynman forces acting on each atom was less than 0.01 eV/Å upon ionic relaxation. The pressure in the unit cell was kept below 5 kbar. Numerical calculations were performed by using the VASP software.²⁵

■ ASSOCIATED CONTENT

Ⓢ Supporting Information

Experimental specifics, materials preparation including MoS₂, MoSe₂, and WSe₂, and Supporting Information on annealing effects. This material is available free of charge via the Internet at <http://pubs.acs.org>.

■ AUTHOR INFORMATION

Corresponding Author

*E-mail: wuj@berkeley.edu.

Author Contributions

¶S.T. and J.Z. contributed equally

Notes

The authors declare no competing financial interest.

■ ACKNOWLEDGMENTS

This work was supported by the U.S. Department of Energy Early Career Award DE-FG02-11ER46796. Part of the materials processing and device fabrication used facilities at the Lawrence Berkeley National Laboratory, which is supported by the Office of Science, Office of Basic Energy Sciences, of the U.S. Department of Energy under Contract No. DE-AC02-05CH11231. We thank Dr. Changyun Ko for his help on nano-Auger measurements.

■ REFERENCES

- (1) Splendiani, A.; Sun, L.; Zhang, Y.; Li, T.; Kim, J.; Chim, C. Y.; Galli, G.; Wang, F. Emerging Photoluminescence in Monolayer MoS₂. *Nano Lett.* **2010**, *10*, 1271.
- (2) Mak, K.; Lee, C.; Hone, J.; Shan, J.; Heinz, T. F. Atomically Thin MoS₂: A New Direct-Gap Semiconductor. *Phys. Rev. Lett.* **2010**, *105*, 136805.
- (3) Zeng, H.; Dai, J.; Yao, W.; Xiao, D.; Cui, X. Valley polarization in MoS₂ monolayers by optical pumping. *Nat. Nanotechnol.* **2012**, *7*, 490.
- (4) Mak, K.; He, K.; Shan, J.; Heinz, T. F. Control of valley polarization in monolayer MoS₂ by optical helicity. *Nat. Nanotechnol.* **2012**, *7*, 494.
- (5) Cao, T.; et al. Valley-selective circular dichroism of monolayer molybdenum disulphide. *Nat. Commun.* **2012**, *3*, 887.
- (6) Radisavljevic, B.; Radenovic, A.; Brivio, J.; Giacometti, V.; Kis, A. Single-layer MoS₂ transistors. *Nat. Nanotechnol.* **2012**, *6*, 147.
- (7) Tongay, S.; Zhou, J.; Ataca, C.; Lo, K.; Matthews, T. S.; Li, J.; Grossman, J. C.; Wu, J. Thermally driven crossover from indirect toward direct bandgap in 2D semiconductors: MoSe₂ versus MoS₂. *Nano Lett.* **2012**, *12*, 5576.
- (8) Ataca, C.; Sahin, H.; Ciraci, S. Stable, Single-Layer MX₂ Transition-Metal Oxides and Dichalcogenides in a Honeycomb-Like Structure. *J. Chem. Phys. C* **2012**, *116*, 8983.
- (9) Yun, W. S.; Han, S. W.; Hong, S. C.; Kim, I. G.; Lee, J. D. Thickness and strain effects on electronic structures of transition metal dichalcogenides: 2H-MX₂ semiconductors (M = Mo, W; X = S, Se, Te). *Phys. Rev. B* **2012**, *85*, 033305.
- (10) Mak, K. F.; He, K.; Lee, C.; Lee, G. H.; Hone, J.; Heinz, T. F.; Shan, J. Tightly bound trions in monolayer MoS₂. *Nat. Mater.* **2012**, *12*, 207.
- (11) Ross, J.; et al. Electrical Control of Truly Two Dimensional Neutral and Charged Excitons in a Monolayer Semiconductor. *Nat. Commun.* **2012**, *4*, 1474.
- (12) Benameur, M. M.; Radisavljevic, B.; Héron, J. S.; Sahoo, S.; Berger, H.; Kis, A. Visibility of dichalcogenide nanolayers. *Nanotechnology* **2011**, *22*, 125706.
- (13) Lee, C.; Yan, H.; Brus, L. E.; Heinz, T. F.; Hone, J.; Ryu, S. Anomalous Lattice Vibrations of Single- and Few-Layer MoS₂. *ACS Nano* **2010**, *4*, 2695.
- (14) Stebe, B.; Ainane, A. Ground state energy and optical absorption of excitonic trions in two dimensional semiconductors. *Superlattices Microstruct.* **1989**, *5*, 545.
- (15) Esser, A.; Runge, E.; Zimmermann, R.; Langbein, W. Photoluminescence and radiative lifetime of trions in GaAs quantum wells. *Phys. Rev. B* **2000**, *62*, 8232.
- (16) Kheng, K.; Cox, R. T.; Merle d'Aubigne, Y.; Bassani, F.; Saminadayar, K.; Tatarenko, S. Observation of Negatively Charged

Excitons X in Semiconductor Quantum Wells. *Phys. Rev. Lett.* **1993**, *71*, 1752.

(17) Warburton, R. J.; Schaefflein, C.; Haft, D.; Bickel, F.; Lorke, A.; Karrai, K.; Garcia, J. M.; Schoenfeld, W.; Petroff, P. M. Optical emission from a charge-tunable quantum ring. *Nature* **2000**, *405*, 926.

(18) Finkelstein, G.; Shtrikman, H.; Bar-Joseph, I. Optical Spectroscopy of a Two-Dimensional Electron Gas near the Metal-Insulator Transition. *Phys. Rev. Lett.* **1995**, *74*, 976.

(19) Huard, V.; Cox, R. T.; Saminadayar, K.; Arnoult, A.; Tatarenko, S. Bound States in Optical Absorption of Semiconductor Quantum Wells Containing a Two-Dimensional Electron Gas. *Phys. Rev. Lett.* **2000**, *84*, 187.

(20) Fang, H.; Chuang, S.; Chang, T. C.; Takei, K.; Takahashi, T.; Javey, A. High-Performance Single Layered WSe₂ p-FETs with Chemically Doped Contacts. *Nano Lett.* **2012**, *12*, 3788.

(21) Kang, J.; Tongay, S.; Zhou, J.; Li, J.; Wu, J. Band offsets and Heterostructures of Two-Dimensional Semiconductors. *Appl. Phys. Lett.* **2013**, *102*, 012111.

(22) Blochl, P. E. Projector augmented-wave method. *Phys. Rev. B* **1994**, *50*, 17953.

(23) Perdew, J. P.; Burke, K.; Ernzerhof, M. Generalized Gradient Approximation Made Simple. *Phys. Rev. Lett.* **1996**, *77*, 3865.

(24) Grimme, S. Semiempirical GGA-type density functional constructed with a long-range dispersion correction. *J. Comput. Chem.* **2006**, *27*, 1787.

(25) Kresse, G.; Hafner, J. Ab initio molecular dynamics for liquid metals. *Phys. Rev. B* **1993**, *47*, 558.